Rheological, Mechanical and Physical Properties of Poly-Lactic Acid (PLA)/ Hydroxyapatites (HA) Composites Prepared by an Injection Moulding Process

Afeeqa Puteri Marzuki, Farrahshaida Mohd Salleh,*
Muhammad Nazri Shah Rosli, Izdihar Tharazi,
Abdul Hakim Abdullah, Nurul Hayati Abdul Halim
School of Mechanical Engineering, College of Engineering,
Universiti Teknologi MARA, 40450 Shah Alam, Selangor, Malaysia
**fshaida@uitm.edu.my*

ABSTRACT

Poly-lactic acid (PLA) is an attractive biopolymer where it is biocompatible with respect to biomedical applications. Hydroxyapatite (HA) ceramics have been broadly practiced as bone substitutes because of their chemical composition close to the mineral phase of bone. Indirectly, the combination of PLA and HA would be a suitable biomaterial candidate for implant and bone repair applications. In this study, the feedstock composition of PLA/HA has been investigated to obtain good rheological properties before undergoing an injection moulding process. The process begins with mixing the specific powder loadings of 60 wt.% PLA/ 40 wt.% HA at 30 rpm of rotating speed and 180 ^{o}C of mixing temperature. Then, the feedstock is evaluated using a capillary rheometer at three different temperatures, 140 ^{o}C, 150 ^{o}C, and 160 ^{o}C. Feedstock exhibiting pseudoplastic flow (n<1) is chosen for the injection moulding process. The result shows injected moulded part successfully produced at barrel and nozzle temperature of 160 ^{o}C, mould temperature of 37 ^{o}C and injection pressure of 0.7 MPa. The injected parts were characterized for physical and mechanical properties. The PLA/HA specimen density is 1.564 ± 0.02 g/cm^{3}. The Young's Modulus of the tensile is 1.82 ± 0.5 GPa within the range of human bone, 1.15 to 5.44 GPa.

Keywords: *Poly-Lactic Acid; Hydroxyapatite; Rheological; Mechanical; Injection Moulding Processing*

ISSN 1823-5514, eISSN 2550-164X

Received for review: 2021-11-19
Accepted for publication: 2022-03-21
Published: 2022-04-15

Introduction

A compostable polymer called polylactic acid (PLA) can be derived from renewable resources, mainly starch and sugar derivates [1]. Besides being a renewable resource, PLA is an eco-friendly biopolymer that is biodegradable, recyclable and compostable [2]. PLA is a promising biopolymer because it has no adverse effects on the environment when used (sustainability) and is not harmful to the ecosystem (earth-friendly) because it does not contaminate water, air or soil. PLA had been developed for medical uses as speciality grade. Its benefits of biocompatibility and being bioresorbable have made it a suitable choice for drug delivery systems, resorbable sutures and blood vessels primarily used in dressing, industry and many more applications [3].

Hydroxyapatite (HA) is one of the usual forms of calcium phosphate. The extraordinary trait of its structure lies in its ability to form strong solutions and to accept an enormous number of anionic and cationic substituents [4]. Additionally, HA ceramics have been broadly used as bone substitutes. It has been the most widely used substitute material for artificial bone grafts for nearly three decades [5]. It also has excellent biocompatibility with tissue bone because its chemical composition is close to the mineral phase of bone. Indirectly, this meets the condition of any materials designed for bone repair and augmentation [6].

The combination between PLA and HA have generated tremendous interest, highlighted as among the most innovative materials being developed especially in biomedical applications. PLA has a drawback as well, which is that it has limited applicability. Besides, PLA has poor toughness where it is a brittle material with less than 10% elongation at break [7]. However, the polymer of PLA is thermoplastic and biodegradable, making it exceptionally desirable by introducing hydroxyapatite (HA). By mixing these two materials, the mechanical and physical properties can be tailored to suit the required properties. It meets the condition of being able to repair bone defects caused by bacterial infections, tumours or bone loss due to trauma [5]. Zare et al. [8] study confirmed that mixing HA into the PLA matrix produced optimum mechanical properties comparable to the human bone. Additionally, after the addition of HA to the PLA, the scaffolds sample becomes bioactive, which results in the cells forming a new bone that is micro environmentally friendly [9]. Moreover, Prakash et al. [10] revealed the cells of the PLA/HA composite had interacted and attached with the other cells during the in vitro experiment, where the work was performed in a test tube. This combination had also shown excellent bioactivity and biocompatibility, which these properties are essential for a bone implant.

Various techniques such as extrusion, hot pressing, electrospinning and 3D printing have been used to process the PLA/HA composite material into the final product. Fabrication of polymer-based medical biomaterials through injection moulding methods is difficult to replace with other technologies,

primarily due to the balance of costs, technological feasibility and material characteristics [11]. Moreover, the injection moulding process can produce small implantable parts with increased complexity in mass production. In this manufacturing technique, the mould temperature, injection temperature, injection speed and injection pressure are the vital parameters for the injection moulding process. These may influence the accuracy and precision of the final specimen [12]. The defect-free product can be produced by setting the injection temperature greater than the melting point of the higher molecular or backbone binder as this temperature affects the melt viscosity and the capability of the materials to fill the cavity. Besides, the mould temperature must be set lower than the melting point and recrystallization temperature of the lower molecular weight binder component or primary binder. Mould temperature influences stress development, cooling rate, and mould cavity filling. Additionally, the injection speed and pressure are important because these ensure fast filling of the die cavity [13].

Over the past few years, the lack of research on PLA/HA composite materials through injection moulding has been studied. HA injection moulding can be injected with a binder consisting of a primary and secondary binder, then will proceed to secondary processing by debinding and sintering to produce the high dense ceramic part [14]. In this study, there is no debinding and sintering process is performed since the injected moulded composite part is the final product. Unexplored study of PLA/HA composite materials through injection moulding process especially for the specific powder loadings of 60 wt.% PLA/ 40 wt.% HA bring about this research. Most of the feedstock compositions covered using the injection moulding process have been between 80 to 95 wt.% PLA and 5 to 30 wt.% HA [11], [15, 16]. Hence, this study focuses on the increment weight percentage of HA, which promises a high bioactivity process and mechanical resistance. Furthermore, the author experimented with high content of HA, which was 40 wt% to determine whether this high content could be promising for the injection process which includes having good flowability of the feedstock.

The main objective of this study is to evaluate the potential use of PLA composites containing HA as an implant material. The work is mainly focused on the influence of high content HA which is 40 wt% on the rheological, mechanical and physical performance of PLA/HA composites. The identification of excellent rheological behaviour is crucial as the viscosity, which links to shear rates and shear stress, will lead to a successful moulding process to produce an injected part without defects. Then, the injected PLA/HA composite was analysed for its mechanical and physical properties and compared with human bone properties.

Methodology

The materials used were poly-lactic acid (PLA) and hydroxyapatite (HA), Sigma Aldrich, where both materials were in the form of powder. First, the particle size distribution of HA powder was analysed using Sigma Aldrich Malvern Instruments (Mastersizer 2000 machine). The thermal analysis using the DSC method was used to evaluate any changes in the PLA materials in melting temperatures. This information is essential in evaluating the quality of the mixture and estimating the temperature to be used during the rheology and injection moulding process. The DSC method uses a Differential Scanning Calorimetry (DSC) machine to measure the transition temperature by following the standard of DSC testing, ASTM D3418. The heating rate was set at 10 °C/min with nitrogen as a purge gas. The gas flow rate was set at 20 ml/min from 25 ^{o}C to 500 °C. FT-IR analysis was conducted using a Fourier Transform Infrared Spectroscopy (FTIR) machine to study the chemical bonding and molecular structure of the PLA and HA powders. The infrared (IR) spectra were recorded between 400 cm^{-1} and 500 cm^{-1} at a resolution of 8 cm^{-1}. Next, the morphology of the HA and PLA particles were observed using a Scanning Electron Microscope (SEM) machine on the PLA and HA powder.

The ratio between PLA and HA powders was prepared according to a specific powder loading of 60 wt.% PLA and 40 wt.% HA. The two powders were blended through a mixing process using the VT Sigma Blade Mixer. The mixing and blending process of PLA/HA was set at a speed of 30 rpm at a temperature of 180 ^{o}C. The prepared composite material of PLA/HA was tested using the rheological test to identify the flowability of the composite material. The testing was carried out using a Rosand Capillary Rheometer machine (Bohlin Instrument RH2000) at three (3) different temperatures, 140 ^{o}C, 150 ^{o}C and 160 ^{o}C. The pressure was set at 0.1 MPa with a maximum shear rate of 5000 s^{-1}. Two significant information were systematically studied: flow activation energy, *Ea* and flow behaviour index, *n.*

The low-pressure injection moulding machine was used to produce tensile specimens as shown in Figure 1. An ideal temperature for injection was 160 ^{o}C based on the rheology characterization with a pressure of 0.7 MPa when injecting the PLA/HA specimens. Every specimen produced was tested for its physical (Archimedes' density, XRD and SEM) and mechanical (tensile) properties. The specimens were analysed for XRD using an X-Ray Diffractometer with parameters of 40 kV of voltage, 40 mA of current and 3 kW of power in the 2θ angle range of 10^{o} until 90^{o} to determine the structure and phases of the PLA/HA specimens [17]. The tensile tests were performed by using a Universal Testing Machine. Each of the specimens used had a thickness of 4.5 mm and 22 mm of gage length, with reference to ASTM D638. The specimens were analysed using SEM to observe the fracture surface after tensile testing.

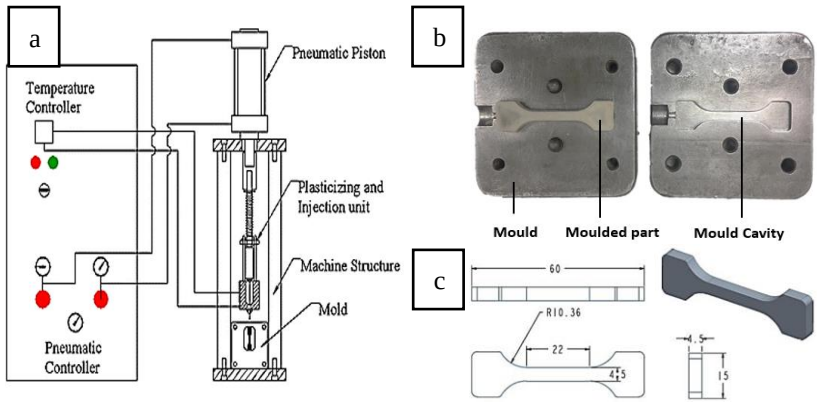

Figure 1: (a) Schematic diagram of manually operated injection moulding machine [18] (b) Mould used to produce tensile specimens (c) Tensile test specimen

Results and Discussion

Material characterization

The DSC result of the PLA is shown in Figure 2. The curves clearly show two peaks concerning the glass transition and melting point. The glass transition temperature (T_g) at 68 ºC is slightly higher than the reported values for PLA, which was 55 ºC. The melting point (T_m) at 168 ºC is within the range of reported values by Farah et al. [19], which was 165 ºC. The difference in T_g values was due to molecular characteristics and molecular weights of PLA material. However, the thermogram of PLA material demonstrated no crystallization peak. This is because this polymer is almost amorphous with low crystalline content (about 3-5 wt%). Besides, the crystallization rate is very slow compared to the DSC scan rate [20]. As a result, the temperature for mixing and blending should be held at or below 181 °C which indicates the proper limit of T_m. The value of T_m was not selected due to the losses in the heat delivery tube which needed to be considered during the mixing. The rheological test temperature and injection temperature needed to be set lower than 168 °C, as seen in the DSC graph.

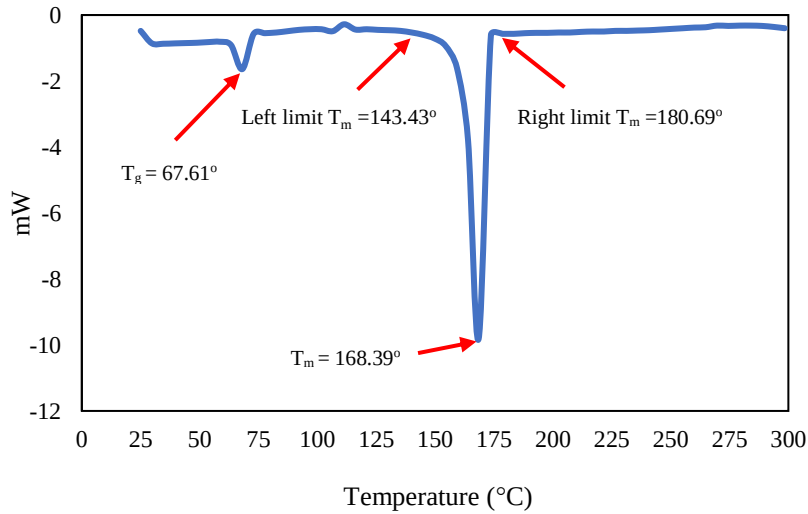

Figure 2: DSC graph of the PLA sample

In addition, FTIR analysis was conducted to check for the presence of functional groups of liquids. Based on Figure 3, the functional groups in the FTIR spectrum of PLA powder were hydroxyl, carbonyl and ether which were represented by the chemical formulae of OH^-, C=O and C–O–C, respectively. The focus regions for the PLA powders sample for the C=O stretch were between 1750 cm^{-1} and 1450 cm^{-1}, while the focus regions for the O–H stretch were between 3600 cm^{-1} and 3200 cm^{-1}. PLA for the C=O stretching and C–O–C stretching was clearly shown at peaks between 1750 cm^{-1} and 1180 cm^{-1}, as represented in the spectra graph. The O–H band for the PLA samples became gradually broader as the fibre substance increased over time. 'Free' hydroxyl bunches may have formed, which were currently occupied with hydrogen bonding [21]. The result obtained for each functional group was in agreement with the researcher, Mofokeng et al. [22], where the range of values of O–H was between 3600 and 3000 cm^{-1} while for the C=O and C–O–C stretching, were 1750 cm^{-1} and 1180 cm^{-1} respectively.

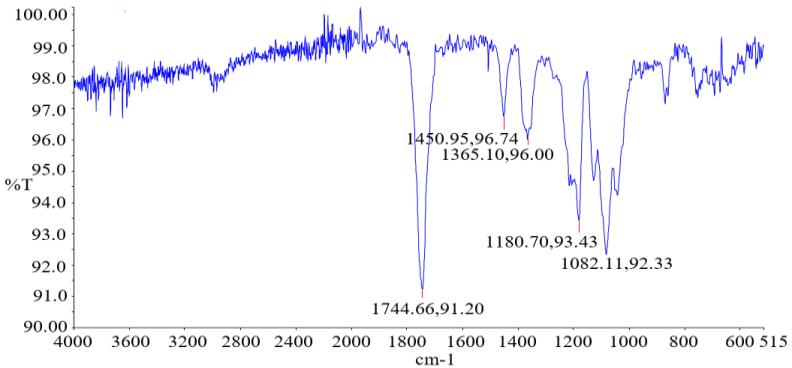

Figure 3: PLA sample spectra graph

Table 1 displays the results of particle size analysis for hydroxyapatite (HA) powders which are measured by the Malvern particle analyser. The size of the particle was 2.69 µm to 30.22 µm. Figure 4 depicts a graph of particle size distributions with bimodal distributions. In this case, a typical bimodal particle size distribution with a bell-shaped distribution can be described as a combination of two ordinary distributions with identical fluctuations but distinct means. If the weights were not the same, the resulting distribution may be bimodal but with peaks of different heights. The crystallinity of PLA and bimodal particle size distribution of HA composites will increase the restriction at the interface between polymer matrix and particle, enhancing the interfacial strength [23]. This statement could be supported by Takayama *et al*. [24], where the research demonstrated that bimodal exhibit the highest values of mechanical properties compared to micro and nano HA by 50% and 10% of elastic modulus and strength, respectively.

Table 1: HA powder properties

Particle name	**Hydroxyapatite (HA) powder**
Weighted residual (%)	1.134
Specific surface area (m^2/g)	1
Concentration (%Vol)	0.0082
Surface weighted mean D [3, 2] (µm)	5.990
Volume weighted mean D [4, 3] (µm)	12.913
Span	3.309
Particle size (µm)	$d_{0.1}$: 2.690
	$d_{0.5}$: 8.320
	$d_{0.9}$: 30.223

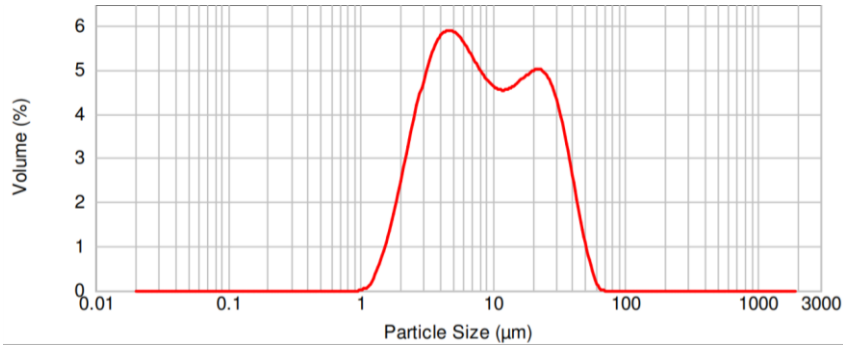

Figure 4: Particle size distribution of HA powder

Figure 5 shows the HA sample graph where the functional groups in the FTIR spectrum of HA powder were hydroxyl, carbonate and phosphate represented by chemical formulae of OH^-, PO_4^{3-}, and CO_3^{2-} respectively. The OH^- band was identified at 3740 and 3620 $cm^{-1,}$ while the CO_3^{2-} stretching was clearly shown in the graph at peaks of 1740 cm^{-1}. This finding was in agreement with previous research where the range was between 3570 and 3427 cm^{-1} for hydroxyl and 1655 cm^{-1} for the carbonate group. The group of PO_4^{3-} stretching frequencies of the HA sample was indicated by 1030, 601 and 562 cm^{-1} in agreement with the study of Raya et al. [25] where the group of PO_4^{3-} was located at 1044, 604, and 565 cm^{-1}.

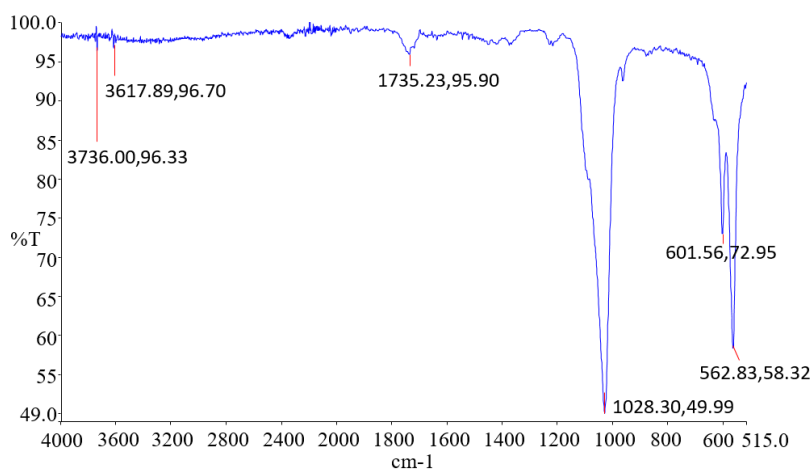

Figure 5: HA sample spectra graph

Figure 6 shows the morphology of PLA and HA powder. The powder particle of PLA was shaped mostly like a rounded potato with a smooth-looking surface/ While, HA powder was agglomeration flakes shape.

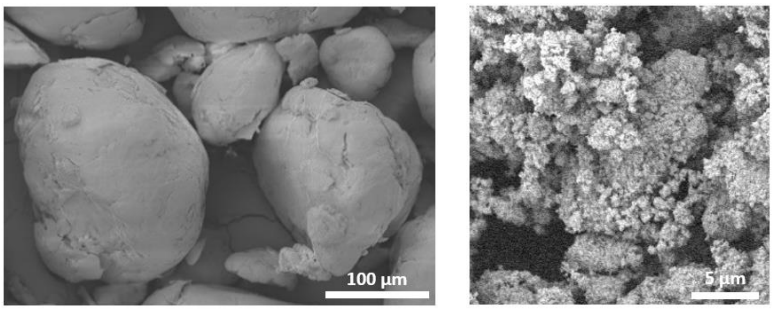

(a) (b)

Figure 6: Morphology structure (a) PLA and (b) HA powder

Rheological properties of PLA/HA

Figure 7 shows the rheological properties of PLA/HA composite material with HA content of 40 wt%. Based on the results, the graph of viscosity and shear rate for the mixture between PLA and HA powders at feedstock temperatures of 140 ºC, 150 ºC and 160 ºC shows pseudoplastic behaviour where the viscosity drops with an increase in shear rate. It shows that it contains polymers at rest which are coiled up due to the stabilizing molecular forces when the shear is applied through mixing. Then, the polymer chains begin to untangle due to agitation and align themselves with the flow and the internal resistance decreases. In 2021, Trotta et al. [26] noted that this flow behaviour leads to less interaction between molecules and particles and a wide amount of free space, which reduces the viscosity. Besides, this kind of behaviour can ease the process of mould filling and minimize jetting [27]. According to the graph, the viscosity and shear rate data series range between 10 to 1000 Pa.s and 100 to 5000 s^{-1}, respectively. In ceramic injection moulding, the maximum viscosity of the required feedstock at moulding temperature is 1000 Pa.s [14]. The result showed PLA/HA composite material was below 1000 Pa.s which is suitable for the injection moulding process.

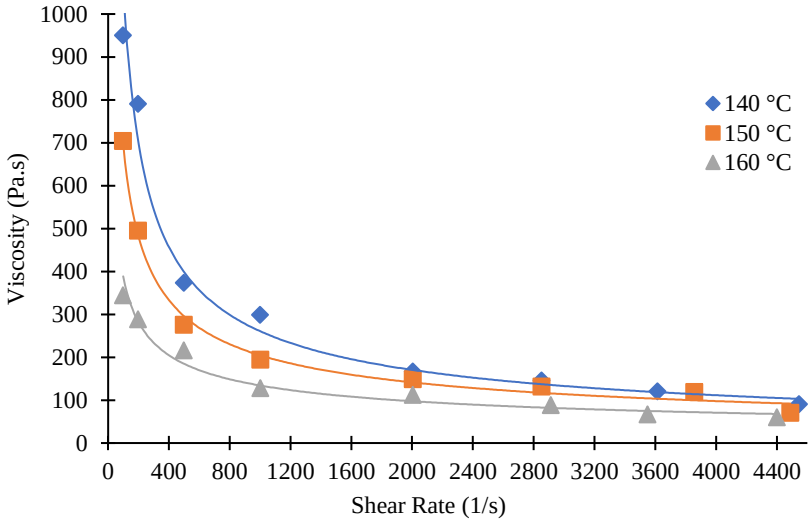

Figure 7: Graph of viscosity vs shear rate for PLA/HA feedstock at three different temperatures

The preferable flow behaviour in the injection moulding process is pseudoplastic. This rheological behaviour can be calculated using the Power-Law equation as referred to Equation (1) where η is viscosity, K is consistence index, γ is shear rate and n is the power-law exponent (flow behaviour index). The value of n for pseudoplastic is below 1 (n<1).

$$\eta = K\gamma^{n-1} \quad (1)$$

Table 2 shows the value of n for the feedstock at a temperature of 140 ^{o}C, 150 ^{o}C and 160 ^{o}C. Based on the result, the n values for all temperatures were below 1 (n<1). The smaller value of the flow behaviour index contributes to high shear sensitivity. Thus, the faster the viscosity and shear rate of the feedstock changed [28]. As a result, the temperatures of 140 ^{o}C, 150 ^{o}C and 160 ^{o}C as tested in the rheometer are suitable for the later process of injection moulding.

Table 2: Flow behaviour index, n for three temperatures

Temperature (^{o}C)	**Flow behaviour index (n)**
140	0.39
150	0.47
160	0.54

During the injection phase, the temperature influences the flow activation energy, *Ea* of the PLA/HA mixture, which can be generalised by using the Arrhenius equation, as seen in Equation (2), where η, η_o, E, R and T are the viscosity of the mixture, viscosity at a particular temperature, flow activation energy, the universal gas constant and temperature (Kelvin), respectively.

$$\eta = \eta_o \exp(E/RT) \quad (2)$$

Based on Figure 8, the data trend of the graph is approaching a straight line for the PLA/HA composite. Using the equation above as a reference for calculation, the value of flow activation energy, *Ea* is 49.54 kJ/mol. Salleh et al. [14] reported the value of *Ea* for the HA/binder system (81.11 wt% HA-11.33 wt% PE/7.55 wt% PS) was 4.34 kJ/mol to 17.97 kJ/mol. Research in 2021 by Besar et al. for PCL/HA composite with HA content (wt%) of 10, 20, 30 and 40 demonstrated *Ea* values of 2.24, 2.56, 3.4 and 4.08 kJ/mol, respectively [29]. This indicates that the higher content of HA leads to a high value of *Ea* and vice versa. In this study, the result obtained for *Ea* was quite high compared to previous research stated. This is due to the effect of the particle size, shape and weight percentage of HA on the rheological behaviour of the PLA/HA composite. A low *Ea* value in a feedstock is a fundamental requirement for the proper powder injection moulding process as the viscosity is not so sensitive to temperature variations. A sudden change of viscosity will result in cracking and distortion defects. Salleh et al. [14] reported that the low *Ea* would produce less feedstock affectability against the temperature where the structure of stress concentration, fracture and defects of the moulded part is reduced.

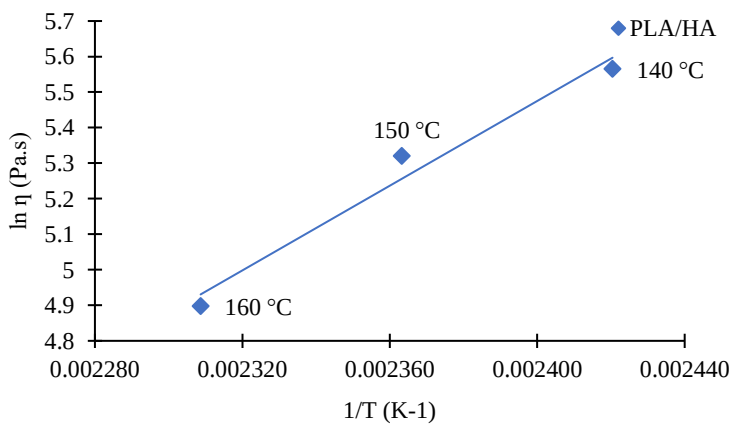

Figure 8: Graph of viscosity against temperature for the PLA/HA feedstock

60 wt% of PLA/ 40 wt% of HA specimen

For the injection moulding process, all the feedstock exhibiting pseudoplastic flow (n<1) was chosen to produce PLA/HA specimens. Based on the rheological analysis, the temperatures of 140 °C, 150 °C and 160 °C proceeded for the injection process as these temperatures exhibited pseudoplastic rheological behaviour.

Figure 9 (a) and (b) show the defects that occurred on the specimen when injected at a temperature of 140 °C. The defect resulted from low pressure as the sample was injected into the mould. If the plastic is too viscous, it can solidify before filling all the cavities, resulting in a short shot. Not only that, even sink marks and flow marks were discovered. Sink marks are often formed when the cooling time required for the feedstock to fully cool and cure while in the mould is insufficient. Besides, it is also caused by inadequate pressure in the cavity or by an excessive temperature at the gate. Then, flow marks formed as a result of a difference in the extent to which cooling occurs upon contact with the mould surface at the front end of the feedstock while the molten feedstock is running within the cavity of the mould [30].

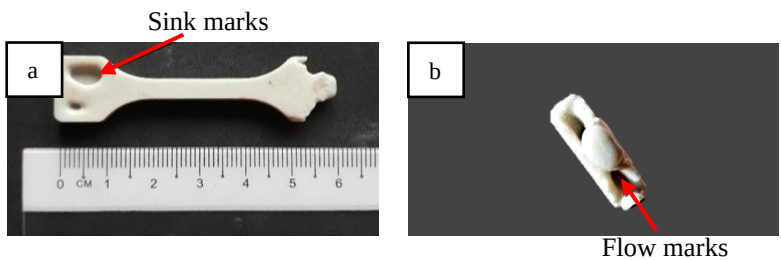

Figure 9: PLA/HA specimen defects at a temperature of 140 ^{o}C (a) Sink marks and (b) Flow marks

Figure 10 (a) shows minor defects such as cracks and flashing when injected at 150 °C. Cracks appearing at the edges or corners of an injected part are due to the manual technique of specimen ejection. As a result of the high ejection force, cracking around the edges of the specimen had occurred as the mould used is without the pin ejector system. Hence, the use of mould with an ejector system can produce a better-quality final part than the system without an ejector. Flash occurs if molten feedstock escapes from the mould cavity through the separating line areas. This always happens when the mould is not clamped tightly enough. According to Huang et al. [31], clamping a mould tightly with the appropriate clamping force will prolong the mould life, minimise energy consumption and avoid defects to the injection moulded parts.

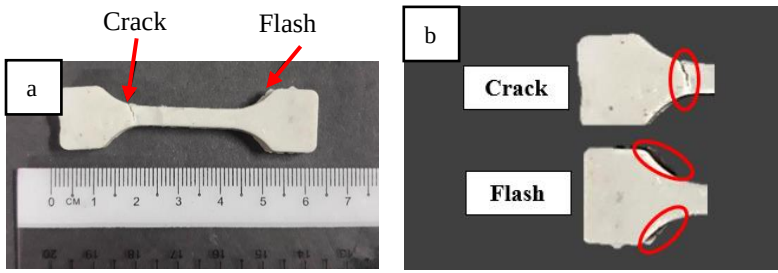

Figure 10: Injected part at 150 °C (a) Minor defects: crack and flash (b) Close-up on the defects

Figure 11 shows injected part produced at a temperature of 160 °C which exhibited excellent and optimized quality on each final part made. This was due to the injection temperature being set depending on rheology temperature analysis, which had pseudoplastic behaviour and was appropriate for the injection procedure. To conclude, the highest viscosity for PLA/HA composite was at 140 °C, hence it can be expected that the feedstock filled into the mould cavity was substantially lower than the two other temperatures. This hypothesis was strengthened by the injected part produced occurred several defects. The lowest viscosity was at 160 °C which the feedstock had filled better into the mould cavity at this temperature. The injected part produced had revealed how the feedstock was filled which is defect-free and high quality.

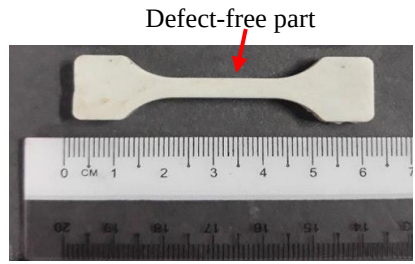

Figure 11: Injected part at 160 °C

Physical properties of PLA/HA

An experimental density test was conducted for the PLA/HA specimen using Archimedes' principle to obtain the physical properties. The average value of density for the PLA/HA specimen was 1.564 ± 0.02 g/cm^3. The theoretical value by applying the rule of mixture for 60 wt% PLA/ 40 wt% HA density was 2.008 g/cm^3. The density obtained was lower than the theoretical value

due to the porosity, small bubbles that exist in the thicker section of injected parts. These pores formed as a result of shrinkage after the material is injected into the mould cavity. Russias et al. [32] discussed the density value is continued to increase from 50 wt% HA to 80 wt% HA and suddenly dropped at 90 and 100 wt% of HA. This is because, at high filler contents, agglomeration tends to occur, deteriorating the filler and resulting in decreasing the mechanical and physical properties of composite materials. The characteristics of HA powder itself tend to agglomerate because of the particle's attraction, such as van der Waals forces and chemical bonds [33]. Composites with such high ceramic content may well not densify as much as those with lower HA loadings due to a lack of adequate polymer to provide a more homogenous matrix. However, the obtained value was still acceptable for a composite bone structure. This finding was in agreement with that of previous research where the density value of 70 wt% PLA/ 30 wt% HA was 1.484 ± 0.002 g/cm^3 [34].

Based on the XRD result in Figure 12, HA peaks at 2θ were 16.62^o (021), 18.93^o (011), 32.14^o (221), 51.04^o (331) and 64.18^o (-264), which related to the usual crystalline diffraction angles of HA due to the structural existence of symmetrical hexagons [35], [36]. Furthermore, diffraction peaks of PLA had been observed between the angle of 15^o to 20^o as reported by Hezma *et al.* [36]. HA has maximum intensities compared to PLA because the diffracted planes which generate this maximum intensity have the most atoms in the tested material unit cell and have the most significant number of electrons.

Additionally, the high content of PLA will have shown more diffraction than those with a low PLA content as this PLA content could affect the crystallinity of HA crystals [37]. The observed results indicated that the PLA and HA combination interacts strongly. The results were obtained from the database of materials known as the International Center for Diffraction Data (ICDD) with Powder Diffraction File (PDF) Card No. 009-0432.

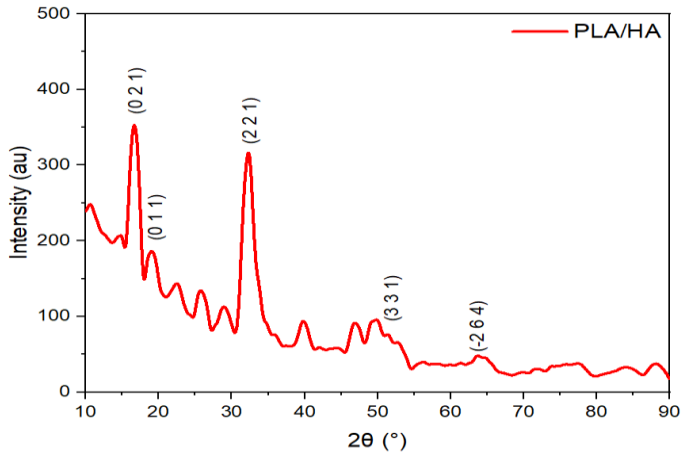

Figure 12: XRD graph for PLA/HA 40%

Mechanical properties of PLA/HA

Figure 13 shows the results of an injected PLA/HA specimen which underwent a tensile test. Based on the graph, two phases had occurred in the stress-strain diagram. The first phase started with the stress occurring once the tensile test begin. Then, the trend becomes constant stress at an average of 5.196 MPa and a strain average of 0.003 to 0.018 which indicates the 'strengthening by straining' process due to plastic deformation with small hardening [38]. This process exhibits the brittle and ductile material which is the composite material of PLA and HA. Based on the curve, the stress remains constant while the strain continues to increase.

The next phase demonstrated the normal deformation. Somehow, the latest deformation process is improved deformation compared to single ductile or single brittle material. This is because the deformation is not only stopped at yield if referred to brittle material and this PLA/HA does not experience curve trending but increases because it still has a hardness that can withstand the stress of load. To conclude, this is the improvement of the composite material that is desired to have high hardness and good ductility which is the combination of ductile and brittle material.

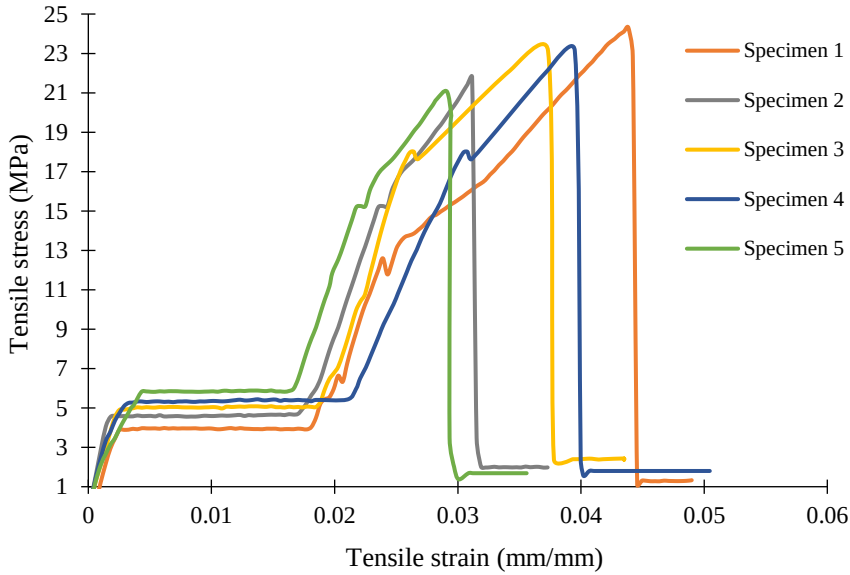

Figure 13: Graph of tensile stress-tensile strain for PLA/HA specimen

Table 3 shows the statistical analysis of the testing. In addition, the average value of the ultimate tensile strength (UTS) was 22.69 ± 1.3 MPa for 40 wt% HA. Ferri et al. [39] reported the value of UTS for PLA/HA composite material decreases from 45.3 MPa (Pure PLA) to 32.6 (30 wt% HA) with a 28% decrease in percentage. This decreasing trend was aligned with the UTS obtained for 40 wt% HA as it should be lower than 32.6 MPa. There might be an interaction between the filler particles and the polymer matrix. According to Zhang et al. [40], the filler acts in two different ways: physically because the particles are very porous, raising surface tension (owing to surface roughness) and chemically because of chemical interactions between the functional groups of PLA and HA. Surface tension rises as a result of chemical reactions. Both elements strengthen the adhesion between the PLA and the HA, and hence the stiffness of the produced composites. Besides, it is known that the tensile strength of a material is an essential determinant of its ability to function in an application as it measures the maximum resistance to fracture [41].

Moreover, the second phase of deformation was considered to calculate the average value of Young's Modulus which is 1.82 ± 0.5 GPa. This is because the value of stress obtained at this phase is significant. This value is in the range of Young's Modulus of human bone, 1.15 ± 0.37 GPa to 5.44 ± 1.25 GPa [42]. Ferri et al. [39] reported the tensile modulus for 0 wt% HA (pure PLA) and 30 wt% HA were 3.93 GPa and 4.63 GPa, respectively. This

demonstrated that as the HA content increases, the Young's Modulus also increases. According to this study, the result of Young's Modulus for PLA/HA composites should be higher than the reported value as the HA content was 40 wt%. However, it can be seen that the Young's Modulus decreased as the HA content increased. This could be related to the possible lowering of the composite capacity of load-bearing after the introduction of HA due to its low flexible nature, hardness and fragile character [43]. It may also have been caused by HA distribution within the PLA matrix and the agglomeration issues as revealed by the SEM images in Figure 15.

In addition, tensile testing showed different values among the specimens. The injection moulding temperature and pressure may have influenced this inconsistency during the specimen preparation. The specimen preparation through the injection moulding temperature needs to be constant because it will affect the agglomerations between the composite materials and lead to inhomogeneous particle distribution [44].

Table 3: Tensile test result for PLA/HA specimen

Specimen	Young's Modulus (GPa)	Yield Strength (MPa)	Ultimate Tensile Strength (MPa)
1	1.60	3.98	24.32
2	2.51	4.60	21.81
3	2.05	4.36	23.13
4	1.39	5.09	23.13
5	1.56	5.81	21.07
Mean	1.82	4.77	22.69
SD	0.5	0.7	1.3

Morphological analysis of PLA/HA

Figure 14 shows the microstructure of the PLA/HA composite with the fracture surface after the tensile testing. The type of fracture which occurred is known as an intergranular fracture, in which the crack was along the grain boundaries. Ferri et al. [39] reported the addition of HA causes a fracture process that resembles a usual fragile fracture. Increasing the filler content had increased the porosity of the composite and, as a result, the capability to absorb energy is significantly reduced. For this composition, HA particles seem to be incorporated in the PLA matrix.

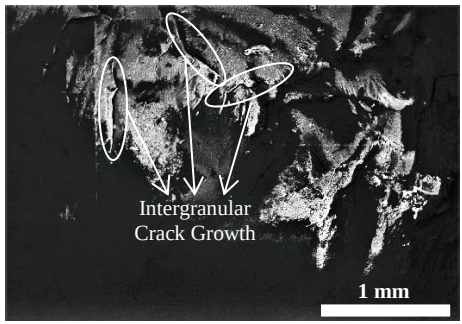

Figure 14: SEM image of fracture surface for PLA/HA

As shown in Figure 15, the SEM image of PLA/HA shows that ceramic (HA) was uniformly distributed within the composites and agglomeration was seen in the composites. Akindoyo et al. [11] revealed that the degree of agglomeration increased when the volume of HA was higher. In this experiment, the volume of HA used was 40 wt% which could be considered high for a ceramic material. This value led to the occurrence of the agglomerations which could act as stress concentration points, which ultimately caused the composite to fail prematurely and affected the characteristics of the composite mechanical. Both agglomeration and porosity formation during the injection moulding process had resulted in poor morphological stability which substantially reduces the activity and lifespan of the supported matrix. As a result, these issues will increase the percentage of failure on the produced composite.

Hence, it can be resolved using a mechanism of particle agglomerate dispersion by ultrasonic cavitation to break up the agglomerated particles [45]. Adding compatibilizer and surface treatment of the filler also could avoid agglomeration [46]. Besides, lowering the value of HA could lead to a decrease in the degree of agglomeration as the ceramic is properly dispersed in the polymer matrix.

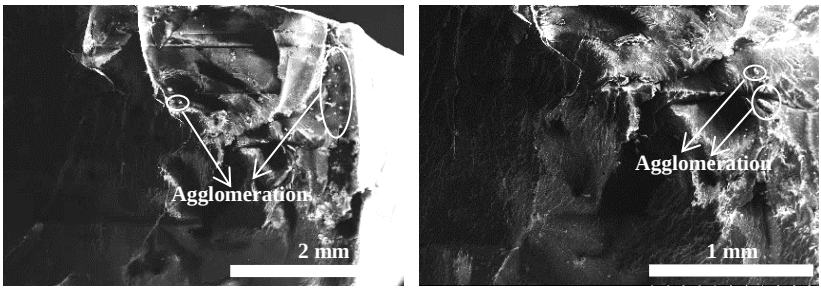

Figure 15: SEM image of PLA/HA

Conclusion

In conclusion, the composites of the PLA and HA were prepared with specific powder loading of 60 wt.% and 40 wt.% respectively through injection moulding. Based on the rheological properties, an optimized feedstock at 160 °C had the best rheological properties which have pseudoplastic behaviour below 1000 Pa.s with a maximum shear rate of 5000 s^{-1}. The Young's Modulus obtained from the injected part of the PLA/HA for the tensile test was 1.82 ± 0.5 GPa. From this study, 40 wt.% of HA content is promised for bone replacement because the value was within the desired range.

Acknowledgement

Acknowledgement is given to the Government of Malaysia and SRP Grant (UI-UiTM BISA) for the financial support under Grant No. 100-RMC 5/3/SRP (049/2021) and College of Engineering, Universiti Teknologi MARA (UiTM), Shah Alam for providing laboratory facilities.

References

[1] R. Datta and M. Henry, "Lactic acid: Recent advances in products, processes and technologies - A review," *Journal of Chemical Technology and Biotechnology*, vol. 81, no. 7. John Wiley & Sons, Ltd, pp. 1119–1129, Jul. 01, 2006, doi: 10.1002/jctb.1486.

[2] D. Henton, P. Gruber, J. Lunt, and J. Randall, "Polylactic Acid Technology," in *Natural Fibers, Biopolymers, and Biocomposites*, CRC Press, 2005.

[3] S. Saeidlou, M. A. Huneault, H. Li, and C. B. Park, "Poly(lactic acid)

crystallization," *Progress in Polymer Science*, vol. 37. no. 12, pp. 1657-1677, 2012, doi: 10.1016/j.progpolymsci.2012.07.005.

[4] B. Zhao, H. Hu, S. K. Mandal, and R. C. Haddon, "A bone mimic based on the self-assembly of hydroxyapatite on chemically functionalized single-walled carbon nanotubes," *Chemistry of Materials*, vol. 17, no. 12, pp. 3235–3241, Jun. 2005, doi: 10.1021/cm0500399.

[5] N. Ramesh, S. C. Moratti, and G. J. Dias, "Hydroxyapatite–polymer biocomposites for bone regeneration: A review of current trends," *Journal of Biomedical Materials Research - Part B Applied Biomaterials*, vol. 106, no. 5. John Wiley and Sons Inc., pp. 2046–2057, Jul. 01, 2018, doi: 10.1002/jbm.b.33950.

[6] L. L. Hench, "Biomaterials: A forecast for the future," in *Biomaterials*, vol. 19, no. 16, pp. 1419–1423, 1998, doi: 10.1016/S0142-9612(98)00133-1.

[7] R. M. Rasal and D. E. Hirt, "Toughness decrease of PLA-PHBHHx blend films upon surface-confined photopolymerization," *Journal of Biomedical Materials Research Part A*, vol. 88, no. 4, pp. 1079–1086, Mar. 2009, doi: 10.1002/jbm.a.32009.

[8] R. N. Zare, E. Doustkhah, and M. H. N. Assadi, "Three-dimensional bone printing using hydroxyapatite-PLA composite," *Materials Today Proceedings*, vol. 42, part. 3, pp. 1531–1533, 2021, doi: 10.1016/j.matpr.2019.12.046.

[9] E. H. Backes *et al.*, "Engineering 3D printed bioactive composite scaffolds based on the combination of aliphatic polyester and calcium phosphates for bone tissue regeneration," *Materials Science and Engineering: C*, vol. 122, pp. 111928, Mar. 2021, doi: 10.1016/j.msec.2021.111928.

[10] C. Prakash *et al.*, "Mechanical Reliability and In Vitro Bioactivity of 3D-Printed Porous Polylactic Acid-Hydroxyapatite Scaffold," *Journals of Materials Engineering and Performance*, vol. 30, pp. 4946-4956, 2021, doi: 10.1007/s11665-021-05566-x.

[11] J. O. Akindoyo, M. D. H. Beg, S. Ghazali, H. P. Heim, and M. Feldmann, "Effects of surface modification on dispersion, mechanical, thermal and dynamic mechanical properties of injection molded PLA-hydroxyapatite composites," *Composites Part A Applied Science and Manufacturing*, vol. 103, pp. 96–105, 2017, doi: 10.1016/j.compositesa.2017.09.013.

[12] N. Hafiez Mohamad Nor, M. Husain Ismail, H. Husain, J. Saedon, M. Azman Yahaya, and S. Alam, "Optimizing Sintering Process to Produce Highest Density of Porous Ti-6Al-4V," *Journal of Mechanical Engineering*, vol. 5, no. 6, pp. 44–55, 2018.

[13] N. N. Mas'ood, A. B. Sulong, N. Muhamad, F. M. Foudzi, and F. M. Salleh, "The study of sintering behavior of stainless steel 17-4ph-stainless steel 316l for two materials powders injection molding (2c-pim) process," *Journal of Mechanical Engineering*, vol. 16, no. 1, pp. 67–77, 2019.

[14] F. Mohd Salleh, Abu Bakar, F. Mohd Foudzi, and I. F. Mohamed, "Flow

Behaviour Characterization of Hydroxyapatite for Powder Injection Moulding (PIM)," *Journal of Mechanical Engineering*, 2017, Accessed: Apr. 17, 2021. [Online]. Available: https://www.researchgate.net/publication/319350932_Flow_Behaviour_Characterization_of_Hydroxyapatite_for_Powder_Injection_Moulding_PIM.

[15] J. O. Akindoyo, M. D. H. Beg, S. Ghazali, and H. P. Heim, "Impact modified PLA-hydroxyapatite composites -Thermo-mechanical properties," vol. 107, pp. 326–333, 2018.

[16] J. M. Ferri, D. L. Motoc, S. F. Bou, and R. Balart, "Thermal expansivity and degradation properties of PLA/HA and PLA/βTCP in vitro conditioned composites," *Journal of Thermal Analysis Calorimetry*, vol. 138, no. 4, pp. 2691–2702, Nov. 2019, doi: 10.1007/s10973-019-08799-0.

[17] Y. Tanimoto and N. Nishiyama, "Preparation and in vitro behavior of a poly(lactic acid)-fiber/ hydroxyapatite composite sheet," *Advances in Materials Science and Engineering*, vol. 2009, 2009, doi: 10.1155/2009/827241.

[18] I. Subuki, Z. Abdullah, R. Razali, and M. H. Ismail, "Rheological study of feed stock for NiTi alloy molded parts," in *IOP Conference Series: Materials Science and Engineering*, vol. 100, no. 1, 2015, doi: 10.1088/1757-899X/100/1/012001.

[19] S. Farah, D. G. Anderson, and R. Langer, "Physical and mechanical properties of PLA, and their functions in widespread applications-A comprehensive review," *Advanced Drug Delivery Reviews*, vol. 107, no. 15, 2016, doi: 10.1016/j.addr.2016.06.012.

[20] S. Fehri, P. Cinelli, M.-B. Coltelli, I. Anguillesi, and A. Lazzeri, "Thermal Properties of Plasticized Poly (Lactic Acid) (PLA) Containing Nucleating Agent," *International Journal of Chemical Engineering and Applications*, vol. 7, no. 2, pp. 85–88, 2016, doi: 10.7763/ijcea.2016.v7.548.

[21] P. K. Bajpai, I. Singh, and J. Madaan, "Development and characterization of PLA-based green composites," *Journal of Thermoplastic Composite Materials*, vol. 27, no. 1, pp. 52–81, 2014, doi: 10.1177/0892705712439571.

[22] J. P. Mofokeng, A. S. Luyt, T. Tábi, and J. Kovács, "Comparison of injection moulded, natural fibre-reinforced composites with PP and PLA as matrices," *Journal of Thermoplastic Composite Materials*, vol. 25, no. 8, pp. 927–948, 2012, doi: 10.1177/0892705711423291.

[23] T. Takayama, K. Uchiumi, H. Ito, T. Kawai, and M. Todo, "Particle size distribution effects on physical properties of injection molded HA/PLA composites," *Advanced Composite Materials*, vol. 22, no. 5, pp. 327–337, 2013, doi: 10.1080/09243046.2013.820123.

[24] T. Takayama, M. Todo, and A. Takano, "The effect of bimodal distribution on the mechanical properties of hydroxyapatite particle filled

poly(L-lactide) composites," *Journal of the Mechanical Behavior of Biomedical Materials*, vol. 2, no. 1, pp. 105–112, Jan. 2009, doi: 10.1016/j.jmbbm.2008.06.001.

[25] I. Raya, E. Mayasari, A. Yahya, M. Syahrul, and A. I. Latunra, "Shynthesis and Characterizations of Calcium Hydroxyapatite Derived from Crabs Shells (Portunus pelagicus) and Its Potency in Safeguard against to Dental Demineralizations," *International Journal of Biomaterials*, vol. 2015, no. 1, 2015, doi: 10.1155/2015/469176.

[26] G. Trotta, B. Stampone, I. Fassi, and L. Tricarico, "Study of rheological behaviour of polymer melt in micro injection moulding with a miniaturized parallel plate rheometer," *Polymer Testing*, vol. 96, pp. 107068, 2021, doi: 10.1016/j.polymertesting.2021.107068.

[27] A. Arifin, A. B. Sulong, N. Muhamad, J. Syarif, and M. I. Ramli, "HA/Ti6Al4V powder with palm stearin binder system - Feedstock characterization," *Applied Mechanics and Materials*, vol. 564, pp. 372–375, 2014, doi: 10.4028/www.scientific.net/AMM.564.372.

[28] R. N. Ahmad, N. Muhamad, A. B. Sulong, A. Wahi, and F. M. Salleh, "Rheological Properties of Titanium Niobium Based Feedstocks for Metal Injection Moulding," *Journal of Mechanical Engineering*, vol. 2, no. 1, pp. 139–149, 2017.

[29] Z. Laja Besar, S. Akhbar, S. Alam, and S. Darul Ehsan, "Effect of particle size, shape, and weight percentage of hydroxyapatite (HA) on rheological behaviour of polycaprolactone/hydroxyapatite (PCL/HA) composites," *Malaysian Journal of Chemical Engineering & Technoogy*, vol. 4, no. 2, pp. 132–136, 2021, doi: 10.24191/mjcet.

[30] V. Piotter, T. Gietzelt, and L. Merz, "Micro powder-injection moulding of metals and ceramics," *Sadhana - Academy Proceedings in Engineering Science*, vol. 28, no. 1–2, pp. 299–306, 2003, doi: 10.1007/BF02717139.

[31] M. S. Huang and C. Y. Lin, "A novel clamping force searching method based on sensing tie-bar elongation for injection molding," *Int. J. Heat Mass Transf.*, vol. 109, pp. 223–230, 2017, doi: 10.1016/j.ijheatmasstransfer.2017.02.004.

[32] J. Russias, E. Saiz, R. K. Nalla, K. Gryn, R. O. Ritchie, and A. P. Tomsia, "Fabrication and mechanical properties of PLA/HA composites: A study of in vitro degradation," *Mater. Sci. Eng. C*, vol. 26, no. 8, pp. 1289–1295, 2006, doi: 10.1016/j.msec.2005.08.004.

[33] X. Ma, Y. Zare, and K. . Rhee, "A Two-Step Methodology to Study the Influence of Aggregation_Agglomeration of Nanoparticles on Young's Modulus of Polymer Nanocomposites _ Enhanced Reader.pdf," *Nanoscale Res. Lett.*, 2017.

[34] N. Monmaturapoj *et al.*, "Properties of poly(lactic acid)/hydroxyapatite composite through the use of epoxy functional compatibilizers for biomedical application," *J. Biomater. Appl.*, vol. 32, no. 2, pp. 175–190, Aug. 2017, doi: 10.1177/0885328217715783.

[35] I. M. Hung, W. J. Shih, M. H. Hon, and M. C. Wang, "The properties of sintered calcium phosphate with [Ca]/[P] = 1.50," *Int. J. Mol. Sci.*, vol. 13, no. 10, pp. 13569–13586, 2012, doi: 10.3390/ijms131013569.

[36] A. M. Hezma, A. B. Abdelrazzak, and G. S. El-Bahy, "Preparation and spectroscopic investigations of hydroxyapatite-curcumin nanoparticles-loaded polylactic acid for biomedical application," *Egypt. J. Basic Appl. Sci.*, vol. 6, no. 1, pp. 1–9, Jan. 2019, doi: 10.1080/2314808X.2019.1586358.

[37] K. Kato, Y. Eika, and Y. Ikada, "In situ hydroxyapatite crystallization for the formation of hydroxyapatite/polymer composites," *J. Mater. Sci.*, vol. 32, no. 20, pp. 5533–5543, 1997, doi: 10.1023/A:1018616306104.

[38] "Mechanics of Materials," 2012. Accessed: Oct. 04, 2021. [Online]. Available: http://www.learncivilengineering.com/wp-content/themes/thesis/images/structural-engineering/Structural-steel-structural-light-gage-reinforcing.pdf.

[39] J. M. Ferri, J. Jordá, N. Montanes, O. Fenollar, and R. Balart, "Manufacturing and characterization of poly(lactic acid) composites with hydroxyapatite," *J. Thermoplast. Compos. Mater.*, vol. 31, no. 7, pp. 865–881, 2018, doi: 10.1177/0892705717729014.

[40] H. ping Zhang *et al.*, "Molecular dynamics simulations on the interaction between polymers and hydroxyapatite with and without coupling agents," *Acta Biomater.*, vol. 5, no. 4, pp. 1169–1181, 2009, doi: 10.1016/j.actbio.2008.11.014.

[41] Ashish, "What Is Ultimate Tensile Strength?," *Science ABC*, 2019. https://www.scienceabc.com/pure-sciences/what-is-ultimate-tensile-strength.html (accessed Nov. 04, 2020).

[42] K. Choi, J. L. Kuhn, M. J. Ciarelli, and S. A. Goldstein, "The elastic moduli of human subchondral trabecular and cortical bone tissue," *J. Biomech.*, vol. 23, no. 11, pp. 1103–1113, 1990, [Online]. Available: http://www.sciencedirect.com/science/article/pii/002192909090003L.

[43] F. Sun, H. Zhou, and J. Lee, "Various preparation methods of highly porous hydroxyapatite/polymer nanoscale biocomposites for bone regeneration," *Acta Biomaterialia*, vol. 7, no. 11. Elsevier, pp. 3813–3828, Nov. 01, 2011, doi: 10.1016/j.actbio.2011.07.002.

[44] M. Maghsoodi and Z. Yari, "Effect of temperature on wet agglomeration of crystals," *Iran. J. Basic Med. Sci.*, vol. 17, no. 5, pp. 344–350, 2014, doi: 10.22038/ijbms.2014.2784.

[45] O. Kudryashova, S. Vorozhtsov, A. Khrustalyov, and M. Stepkina, "Ultrasonic dispersion of agglomerated particles in metal melt," *AIP Conf. Proc.*, vol. 1772, no. October 2016, 2016, doi: 10.1063/1.4964535.

[46] S. M. Nainar, S. Begum, M. N. M. Ansari, and H. Anuar, "Tensile Properties and Morphological Studies on HA/PLA Biocomposites for Tissue Engineering Scaffolds," *Int. J. Eng. Res.*, vol. 3, no. 3, pp. 186–189, 2014, doi: 10.17950/ijer/v3s3/312.